Driven Motion of Vortices in Superconductors*

G.W. Crabtree,[1] G.K. Leaf,[2] H.G. Kaper,[2] V.M. Vinokur,[1]
A.E. Koshelev,[1] D.W. Braun,[2] and D.M. Levine[2]

[1]*Materials Science Division*
[2]*Mathematics and Computer Science Division*
Argonne National Laboratory, Argonne, Illinois 60439

Submitted for publication for the US-Polish Joint Commission on Science and Technology, September 11-15, 1995, Wroclaw, Poland, Springer-Verlag "Lecture Notes in Physics" series, sponsored by US-Polish Marie Sklodowska-Curie Joint Fund II

*Work supported by the U.S. Department of Energy under contract #W-31-109-ENG-38, through the Office of Basic Energy Sciences-Materials Sciences (GWC, VMV) and through the Office of Computational and Technology Research-Mathematical, Information, and Computational Sciences Division subprogram (GKL, HGK, DWB, DML); and by the National Science Foundation-Office of Science and Technology Centers for Superconductivity under contract #DMR91-20000 (AEK).

Driven Motion of Vortices in Superconductors

G. W. Crabtree,[1] G. K. Leaf,[2] H. G. Kaper,[2] V. M. Vinokur,[1]
A. E. Koshelev,[1] D. W. Braun,[2] and D. M. Levine[2]

[1] Materials Science Division
[2] Mathematics and Computer Science Division
Argonne National Laboratory, Argonne, IL 60439 USA

Abstract. The driven motion of vortices in the solid vortex state is analyzed with the time-dependent Ginzburg-Landau equations. In large-scale numerical simulations, carried out on the IBM Scalable POWERparallel (SP) system at Argonne National Laboratory, many hundreds of vortices are followed as they move under the influence of a Lorentz force induced by a transport current in the presence of a planar defect (similar to a twin boundary in $YBa_2Cu_3O_7$). Correlations in the positions and velocities of the vortices in plastic and elastic motion are identified and compared. Two types of plastic motion are observed. Organized plastic motion displaying long-range orientational correlation and shorter-range velocity correlation occurs when the driving forces are small compared to the pinning forces in the twin boundary. Disorganized plastic motion displaying no significant correlation in either the velocities or orientation of the vortex system occurs when the driving and pinning forces are of the same order.

1 Introduction

The driven motion of vortices in superconductors is now attracting substantial interest for its scientific and technological value [1]–[17]. Scientifically, vortices provide a well defined system of interacting strings or pancakes, which can form a liquid, lattice, or disordered glass in equilibrium. Each vortex can be subjected to a controllable external force—the Lorentz force, $\mathbf{F}_L = \mathbf{J} \times \Phi/c$—through the application of a transport current $\mathbf{J}$. (Φ is a vector, whose magnitude is equal to the flux quantum, oriented parallel to the local magnetic induction, $\mathbf{B}$.) This external Lorentz force is resisted by the pinning forces, which arise from material defects and act on the vortices. The defects may be point defects, line defects, or planar defects, and they may be naturally present or artificially induced. The interplay of pinning, interaction, and driving forces, operating within the various phases, leads to richly detailed dynamics and many new and interesting dynamic phenomena. One of the experimental attractions of vortices as a dynamical system is the extensive control over the relevant parameters. For example, the density of vortices can be changed by several orders of magnitude by a simple change in the applied field, the driving force can be controlled through the transport current, and the pinning forces can be varied by controlled irradiation with electrons, protons, neutrons, or heavy ions.

On the technological side, vortex dynamics plays a central role in the success of superconducting applications. Elementary electrodynamics requires that vortex motion be associated with energy dissipation, a detrimental feature for practical use of superconductors. If superconductors are to find extensive applications, the dynamics of vortices must be understood as a prerequisite to prevention and control of dissipation.

The nature of vortex motion differs in each of the equilibrium states. In the liquid state, the shear modulus is zero, allowing neighboring vortices to slide past each other with finite relative velocity. The velocity change between neighboring vortices is controlled by the shear viscosity and is described by a suitable form of hydrodynamics [18]. In the solid state, the motion of vortices is dramatically different. The finite shear modulus prevents the relative shear motion of neighboring vortices by imposing an elastic energy penalty on shear distortions. Consequently, the average velocity of neighboring vortices is identical as long as the elastic limit of the shear modulus is not exceeded. Local elastic distortions may occur, but the shear modulus prevents these distortions from growing because the elastic energy cost becomes too great. The motion may be described by an average velocity of the vortex system, with local elastic fluctuations relative to this average velocity. This *elastic motion* is a continuous process and can be described by a set of partial differential equations involving the elastic displacements of the moving lattice.

When the shear yield stress of the vortex lattice is exceeded, the shear forces are too strong to be accommodated elastically, and another type of solid-state motion occurs which is qualitatively different from elastic motion. The elastic bonds between vortices are broken, and neighboring vortices can have different velocities in the steady state. Remarkably, the velocity differences are not spread over many vortex spacings by viscous processes as in the liquid. Rather, discontinuities in the velocity profile occur, which cannot be described by the usual partial differential equations of hydrodynamics or elasticity theory. We refer to this kind of motion, where a given vortex may see different neighbors during the course of the motion, as *plastic motion.* Plastic motion has recently been recognized experimentally [3]–[5], [8], [10]–[12], [15] and theoretically [1, 2, 6, 7, 9, 16, 17] as a fundamentally important feature of driven vortex dynamics.

In this paper we explore the nature of driven motion of the vortex solid. We present results of numerical simulations of vortex motion near a planar defect, like a twin boundary in $YBa_2Cu_3O_7$, showing important fundamental characteristics of both plastic and elastic motion. We show how the the driven motion of a vortex solid evolves from organized plastic motion at low driving forces, where the planar defect presents a barrier to vortex motion, to disorganized plastic motion at intermediate driving forces, and finally to elastic motion at high driving forces. The defining characteristics of each type of motion revealed by the simulations are compared and discussed.

2 Numerical Simulations

The numerical simulations presented here are based on the time-dependent Ginzburg-Landau (TDGL) equations of superconductivity. These equations, first written down by Schmid [19], were critically analyzed in the context of the microscopic Bardeen-Cooper-Schrieffer theory by Gor'kov and Eliashberg [20]. In the zero-electric potential gauge, they may be summarized as follows:

$$\frac{\hbar^2}{2m_s D}\frac{\partial \psi}{\partial t} = -\frac{\delta \mathcal{L}}{\delta \psi^*}, \quad \frac{\sigma}{c^2}\frac{\partial \mathbf{A}}{\partial t} = -\frac{\delta \mathcal{L}}{\delta \mathbf{A}} - \frac{1}{4\pi}\nabla \times \nabla \times \mathbf{A}, \tag{1}$$

where $\mathcal{L}$ is the density of the Helmholtz free-energy functional,

$$\mathcal{L} = a|\psi|^2 + \frac{b}{2}|\psi|^4 + \frac{1}{2m_s}\left|\left(\frac{\hbar}{i}\nabla - \frac{e_s}{c}\mathbf{A}\right)\psi\right|^2. \tag{2}$$

Here, ψ is the complex order parameter, and $\mathbf{A}$ the vector potential; the other symbols have their usual meaning. Vortices are identified with zeros of the order parameter. We use link variables to preserve gauge invariance in the discretization of the field equations; details of the approximation procedure and the computational method can be found in [21].

The simulations refer to a superconducting slab, infinite and homogeneous in the z direction, periodic in the y direction, and finite in the x direction. The unit of length in all calculations is the penetration depth, λ. A magnetic field is applied in the positive z direction, so the problem is essentially two-dimensional. The superconductor occupies a rectangular region measuring 32×48 (units of λ) in the (x, y) plane. Periodicity is imposed in the y direction. A transport current is applied in the positive y direction, so the Lorentz force is in the positive x direction. At the free surfaces, the boundary condition is $\mathbf{J}_s \cdot \mathbf{n} = 0$, where $\mathbf{J}_s$ is the supercurrent density and $\mathbf{n}$ the normal unit vector.

The transport current is induced by applying a magnetic field $H_l = H + \Delta H$ at the left, $H_r = H - \Delta H$ at the right free surface, where $\Delta H > 0$. Ampère's law requires a current (per unit length in z) of magnitude $J = 2(c/4\pi)\Delta H$ in the y direction.

We take $\kappa = 4$ and adopt a grid of 256×384 mesh points. (κ is the Ginzburg-Landau parameter, $\kappa = \lambda/\xi$, where λ is the penetration depth, ξ the coherence length.) Thus, two mesh widths correspond to one coherence length. No thermal fluctuations are included, so the simulations reflect the motion of the vortex solid.

The twin boundary is simulated as a planar slab, two coherence lengths thick, parallel to the z-axis and making an angle of 45° with the sample boundaries. This geometry, often encountered in single crystals of $YBa_2Cu_3O_7$, was inspired by the interesting barrier effects observed in magneto-optical images of twinned crystals [17], [22]–[27]. The twin boundary is modeled by locally reducing the

condensation energy, with random Gaussian fluctuations to provide the experimentally observed pinning opposing vortex motion within the plane [28]. The average condensation energy in the twin boundary is 56% of the bulk value, and the standard deviation of the fluctuations is 25% of the bulk value.

The computational procedure during each simulation was as follows. First, a small field was applied, to establish the Meissner state. After 200 time steps, the field was increased suddenly to $1.13H_c$, to bring the system into the vortex state. Simultaneously, a transport current was imposed by adjusting the applied magnetic field on either side of the slab. Simulations were run with three transport currents—referred to hereafter as *weak*, *intermediate*, and *strong*—corresponding to approximately 2%, 4%, and 8% of the depairing current. The time-dependent Ginzburg-Landau equations were iterated for 1.832×10^6 time steps, to establish the steady state. At that point, all transient effects had been eliminated, and data recording was initiated. The equations were iterated for an additional 0.580×10^6 time steps, and the values of the order parameter and vector potential at each grid point were recorded at regular time intervals. The number of vortices throughout the recording period was 455, 561, and 651 for the weak, intermediate, and strong current, respectively, with a variation of less than 1% in each case.

The simulations were carried out on the IBM Scalable POWERparallel (SP) system at Argonne National Laboratory (128 processors, 128 Mbytes per processor, theoretical peak performance 16 Gflops). On 16 processors, a simulation of 2.412×10^6 time steps required approximately 100 hours.

The output of a simulation is a sequence of snapshots showing the time evolution of the order parameter, vector potential, and other calculated quantities at each grid point. The spatial variation of the order parameter is analyzed at each time step, to determine the positions of the vortices. The aggregate of these positions over time yields the vortex trajectories during the period of observation. On such a trajectory plot, a moving vortex appears as a line whose length and direction indicate its average velocity.

3 Results

3.1 Weak Current

Figure 1 shows the positions of the vortices for the weak current case for one of the time steps, after steady state has been reached. Delaunay triangulation is shown to highlight the structure of the vortex pattern. The location of the twin boundary is marked by the diagonal dotted line ending near the upper right corner. The vortex system is highly ordered spatially, as expected for a system in the solid state. The lattice structure accommodates the twin boundary

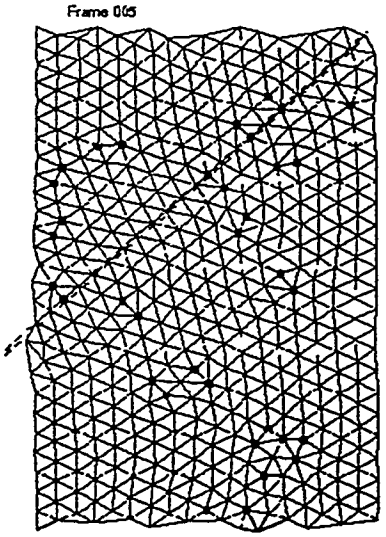

Figure 1: Delaunay triangulation of the vortex positions for one time step in the observation period at weak current. Open and solid circles mark the positions of vortices with five and seven neighbors, respectively.

by orienting one of its close-packed directions with the boundary plane. This is natural, since the lower condensation energy on the twin boundary attracts vortices, making it energetically favorable to maximize the local density. The incommensurablity between the density of vortices on the twin boundary and in the bulk is resolved by dislocations adjacent to the twin boundary.

The accommodation of the structure to the twin boundary conflicts with another accommodation to the right and left edges of the sample [29]. The competition can be seen clearly in Figure 1, where the close-packed directions shift from parallel to the twin boundary near the twin boundary to parallel to the edges near the edges. The shift in orientation of 15° is accommodated by defects in the vortex lattice structure, indicated in Figure 1 by solid or open circles at vortices with seven or five neighbors, respectively. The orientation may shift abruptly, as near the left edge just above the twin boundary, or gradually, as in the center of the sample.

The trajectories of the vortices in weak current are shown in Figure 2. The vortices in the twin boundary are stationary, being pinned against motion parallel or perpendicular to the boundary plane by the random potential. Thus, at weak currents the twin boundary is an impenetrable barrier to vortex motion. The motion occurs external and parallel to the boundary, illustrating a form of

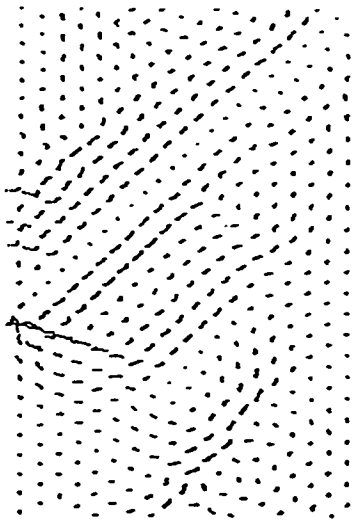

Figure 2: Vortex trajectories at weak current.

twin boundary guidance explained in detail in [17]. At weak current, the twin boundary dominates both the local structure and the motion of vortices.

Close examination of Figure 2 reveals that vortex motion occurs primarily along the close-packed directions of the lattice. This feature is a key element in understanding plastic vortex motion and we will use it often in the following discussion. In particular, it plays an essential role in creating the guided motion that occurs in Figure 2. The guided motion occurs because (i) the twin boundary defines the close-packed directions in the driven vortex system, (ii) this orientational order persists over long range, up to the dimension of the simulated sample, and (iii) vortex motion is restricted to the close-packed directions. It is the combination of all these elements which allows the twin boundary to determine the velocity direction of vortices at distant points. If these elements are absent, the guided motion is severely inhibited or missing, as will be demonstrated explicitly by the results at intermediate current.

A second characteristic feature of Figure 2 is the occurrence of velocity discontinuities. These discontinuities are most obvious at the twin boundary, where the velocity suddenly jumps from zero to approximately its highest value in one lattice spacing. This is quite different from the hydrodynamic motion of liquids, where the velocity profile grows monotonically from zero at the boundary, reaching its highest value deep in the liquid. Additional discontinuities occur in Figure 2 far from any local structural feature. Four rows above the twin

boundary, the velocity abruptly jumps from a high value to nearly zero, and there are discontinuous velocity changes two rows and seven rows below the boundary. Farther below the twin boundary, after a region of little or no motion, two adjacent rows of vortices suddenly flow at substantial velocity parallel to the twin boundary. The discontinuities associated with these two rows have no apparent communication with the twin boundary or with the guided motion adjacent to the boundary. They illustrate the collective nature of the plastic response of the vortices to the particular driving and pinning forces in the simulation.

The plastic motion in Figure 2 displays velocity discontinuities of *direction* as well as *magnitude*. Near the left edge of the sample, just below the twin boundary, there are several rows of vortices moving to the lower right with substantial speed. These vortices border on another group moving to the upper right with approximately equal speed. The discontinuity in direction is dramatic: the velocity change occurs in one vortex spacing with no transition region.

This velocity direction discontinuity may be understood in terms of the principle of motion restricted to close-packed directions. The lattice accommodates the twin boundary by orienting one of its close-packed directions along the boundary, as described above. Since the twin boundary is a barrier to vortex flow, the other two close-packed directions are effectively blocked as paths for motion. If any motion is to occur, it must be along the close-packed direction parallel to the twin boundary. However, just below the left end of the twin boundary, the barrier effect is absent, and all close-packed directions are available for vortex motion. The vortices choose to move to the lower right, because it is the close-packed direction oriented nearest to the direction of the Lorentz force.

Despite the velocity discontinuities, there is a great deal of correlation in the vortex motion in Figure 2. The four rows of vortices above the twin boundary move with approximately equal average velocity, as do the two rows just below the boundary and the fifth to seventh rows below. These correlations of neighboring velocities are easy to understand qualitatively as an effect of the shear modulus. Elastic energy is minimized if neighboring vortices move at the same velocity, so that the shear bonds are not stretched. In spite of this mechanism, the velocity correlations are relatively short range, extending less far than the orientational correlation of the lattice.

Summarizing the observations at weak current, the observed plastic motion is highly organized in several ways. It respects the local structure of the lattice by restricting motion to the close-packed directions. This restricted motion maintains the long-range orientational order of the lattice, while breaking the long-range translational periodicity. The motion is further organized by a high correlation of velocities extending over relatively short ranges compared to the range of orientational correlation. The regions of highly correlated velocity locally minimize the elastic shear energy and terminate suddenly in velocity

discontinuities of both magnitude and direction. Finally, the motion is collective, each vortex coordinating its movements with others to minimize the configurational energy through maintaining long-range orientational order and, to a lesser extent, local translational periodicity.

3.2 Intermediate Current

A qualitatively different kind of plastic motion occurs at intermediate current, shown in Figure 3. Here the twin boundary pinning forces are comparable with

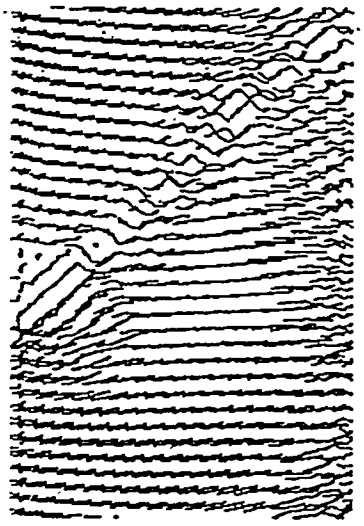

Figure 3: Vortex trajectories at intermediate current.

the driving forces, and the vortices in the boundary are no longer stationary. A new kind of guidance occurs, where vortices move parallel to the boundary but internal to it [17]. This internal guidance is most easily seen at the lower left of the twin boundary, but it also occurs elsewhere along the boundary over shorter distances. Internal guidance occurs in regions of the boundary where the random pinning wells are relatively deep compared to the bulk, but comparable in depth to neighboring wells. The driving force is sufficient to overcome the relatively low local barriers between wells, but insufficient to overcome the larger barriers blocking access to the bulk.

The high correlation among vortex trajectories near the twin boundary, which was apparent at weak current, is missing in Figure 3. There are crossing trajectories in the twin boundary, which indicate that different vortices do not necessarily follow the same path when encountering the same pinning configuration

at different times. Their motion depends not only on the pinning configuration, but also on the local vortex configuration at the time of the encounter.

In Figure 3 the boundary has lost its structure, no longer appearing as an extended object to the vortices. Rather, it is a line of random pinning wells, some of which are strong enough to trap vortices and some of which are too weak to do so. Without local structure, there are no well-defined close-packed directions and no structural features to guide the motion of vortices. The randomness associated with the relative sizes of the pinning and Lorentz forces at intermediate current destroys the coherence of the boundary and is ultimately responsible for the disorder which characterizes the plastic motion in Figure 3. If there is no random element, as in the bulk of the sample where there is no pinning, the motion is highly ordered.

Far from the twin boundary, where pinning is absent, a new order appears in the vortex motion. Figure 3 shows a remarkable uniformity in the vortex trajectories. The vortices all move in nearly the same direction with the same speed. Further, the direction of motion is nearly the Lorentz force direction, not the twin boundary direction. This is quite different from the situation at weak current, where the direction of motion is determined by the close-packed directions and the velocities showed many discontinuities in magnitude. The motion of Figure 3 is the beginning of elastic motion, where all vortices move with the same average velocity. The effect of the twin boundary on the vortex velocities is greatly reduced from that at weak current. There is only local influence in the vicinity of the twin boundary, and it upsets the elastic order imposed by the Lorentz force, rather than defining the orientational order which controls the Lorentz force. Intermediate current represents competition between the Lorentz force and the pinning forces. Neither is dominant, and the unstructured velocities of the vortices near the twin boundary reflect the incoherent nature of their response.

3.3 Strong Current

The vortex trajectories (during the first one-fifth of the observation period) at strong current are shown in Figure 4. The Lorentz force dominates the pinning forces. The direction of motion of the vortices is primarily parallel to the Lorentz force, even in the vicinity of the twin boundary. The internal motion in the twin boundary is gone, except for a small section near the left edge of the frame. Elsewhere, vortex velocities deviate only slightly as they routinely break through the boundary. The plastic motion that occurred at the twin boundary at intermediate current is nearly completely replaced by elastic motion. The boundary no longer interrupts the orderly pattern of the trajectories that occurs on either side, as it does at intermediate current, where the uniform velocity pattern does not continue across the boundary. Here, the trajectories can be traced across the boundary, making the elastic motion across the boundary coherent.

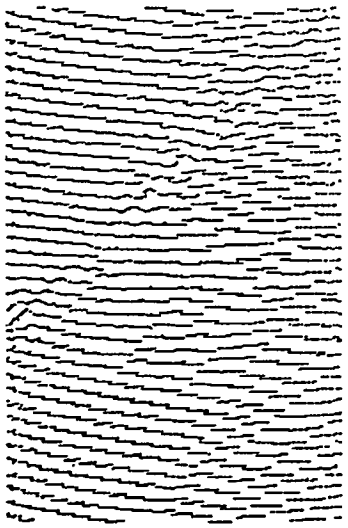

Figure 4: Vortex trajectories during the first one-fifth of the observation period at strong current. Partial trajectories are shown for clarity, to avoid including so many lines that the paths of individual vortices cannot be followed.

4 Discussion and Conclusions

The simulations at weak, intermediate, and strong current reveal several important features of plastic and elastic motion in the presence of extended defects. Two types of plastic motion have been identified: organized motion, where the twin boundary defines the orientational and dynamic structure of the vortex lattice over long distances, and disorganized motion, where there are no long-range correlations in the positions or velocities of the vortices. The key feature determining the kind of plastic motion which occurs is the relative strength of the driving Lorentz force and the opposing pinning forces. When the pinning forces dominate, the twin boundary appears as an extended defect which establishes the orientation of the vortex lattice by defining the close-packed directions. The orientation so defined extends over a long range. The simulations reveal that motion within the lattice structure is restricted to the close-packed directions. This key characteristic explains many of the features of organized plastic flow. Near the twin boundary, two of the close-packed directions are blocked by the barrier effect of the boundary, leaving only one available direction for motion. This produces the guided motion of vortices by the boundary. Because the vortex solid maintains the close-packed directions defined by the twin boundary over long distances, the predominant direction of motion is parallel to the boundary over the whole frame.

The simulations demonstrate discontinuities in the magnitude and direction of the velocities of vortices in plastic motion. The directional discontinuities are controlled by the principle of motion along close-packed directions. They occur

at the end of the twin boundary, where the barrier effect suddenly disappears, and are equivalent to an exchange of one close-packed direction for another which is more nearly aligned with the Lorentz force direction. Discontinuities in the magnitude of the velocity separate regions of correlated motion, containing vortices which move with approximately the same average velocity. The size of these regions is a measure of the velocity correlation length, which is intermediate between the intervortex spacing and the size of the simulated sample. By contrast, the orientational correlation length, which is revealed in the Delaunay triangulation, is substantially longer than the velocity correlation length and is comparable to the size of the simulated sample.

In disorganized plastic motion, both the orientational and velocity correlation lengths are comparable to or shorter than the intervortex spacing. As a result, there is little or no effective correlation. Discontinuities in magnitude and direction of the vortex velocities occur on neighboring vortices, and there is no apparent structure discernible in the vortex trajectories. Vortex velocities include many directions, rather than only the close-packed directions as in organized plastic flow. These qualitative differences from organized plastic flow have their origin in the breakdown of the local structure imposed by the twin boundary. At intermediate current, the driving Lorentz force is strong enough to overcome some of the pinning forces, destroying the extended nature of the twin boundary. The boundary is not capable of defining a local structure for the vortices, so there are no close-packed directions to define the orientation of the vortex system or the allowed directions of vortex motion. We propose that disorganized plastic motion is a result of a random element in the pinning configuration. Here, the random element is the pinning strength which, at intermediate current, competes with the Lorentz force for dominance over the vortex motion. Randomness in the position of pinning sites also produces disordered plastic motion [30]. At lower or higher current, the random element is missing, because the Lorentz force is either decisively smaller or larger than the pinning forces, and a more ordered driven state appears.

The most ordered of all the driven solid vortex states is elastic motion, which occurs at strong current. Here, both the position and velocity correlation are of longer range than the simulated sample size. Translational periodicity as well as orientational order are preserved in the moving lattice. Elastic motion occurs when the Lorentz force dominates the pinning forces. The velocity direction is the Lorentz force direction, a feature that does not occur in either type of plastic motion. The principle of motion along close-packed directions, which defined many of the features of organized plastic motion, can be seen in elastic motion as well. The lattice has re-oriented to make the Lorentz force direction a close-packed direction.

The large-scale time-dependent Ginzburg-Landau simulations presented here demonstrate a powerful new tool for exploring the nature of driven motion of vortices. Parallel processing provides the capability to track the simultaneous

motion of hundreds of vortices, sufficient to observe the discontinuities and correlations which characterize the plastic and elastic flow patterns in the vortex solid. The simulations provide complete microscopic information on position and velocity, which cannot be obtained experimentally. This type of detailed information allows thorough statistical analyses to explore new concepts like dynamic correlation lengths and their relation to the defining parameters of the system, such as the pinning configuration and the driving Lorentz force. Simulations building on the results presented here can be expected to provide important new insights into the nature of dynamic vortex states.

We thank W. K. Kwok and U. Welp for many productive and stimulating discussions. This work was supported by the U.S. Department of Energy under contract #W-31-109-ENG-38, through the Office of Basic Energy Sciences–Materials Science (GWC, VMV) and the Office of Computational and Technology Research–Mathematical, Information, and Computational Sciences Division subprogram (GKL, HGK, DWB, DML) and by the U.S. National Science Foundation Science and Technology Center for Superconductivity under contract #DMR 91-20000 (AEK).

References

[1] A. Brass, H. J. Jensen, and A. J. Berlinsky, Phys. Rev. B **39** 102 (1989).

[2] S. N. Coppersmith and A. J. Millis, Phys. Rev. B **44** 7799 (1991).

[3] S. Bhattacharya and M. J. Higgins, Phys. Rev. B **49** 10005 (1994).

[4] W. K. Kwok, J. A. Fendrich, C. J. van der Beek, and G. W. Crabtree, Phys. Rev. Lett. **73** 2614 (1994).

[5] G. D'Anna, M. V. Indenbom, M.-O. Andre, and W. Benoit, Europhys. Lett. **25** 225 (1994).

[6] R. Kato, Y. Enomoto, and S. Maekawa, Physica C **227** 387 (1994).

[7] A. E. Koshelev and V. M. Vinokur, Phys. Rev. Lett. **73** 3580 (1994).

[8] A. C. Marley, M. J. Higgins, and S. Bhattacharya, Phys. Rev. Lett. **74** 3029 (1995).

[9] A. I. Larkin, M. C. Marchetti, and V. M. Vinokur, Phys. Rev. Lett. **75** 2992 (1995).

[10] P. Thorel, R. Kahn, Y. Simon, and D. Cribier, Journal de Physique **34** 447 (1973).

[11] U. Yaron, P. L. Gammel, D. A. Huse, R. N. Kleiman, C. S. Oglesby, E. Bucher, B. Batlogg, D. J. Bishop, K. Mortensen, and K. N. Clausen, Nature (London) **376** 753 (1995).

[12] J. M. Harris, N. P. Ong, R. Gagnon, and L. Taillefer, Phys. Rev. Lett. 74 3684 (1995).

[13] G. Blatter, M. V. Feigel'man, V. B. Geshkenbein, A. I. Larkin, and V. M. Vinokur, Rev. Mod. Phys. 66 1125 (1995).

[14] L. Balents and M. P. A. Fisher, preprint.

[15] A. Duarte, E. F. Righi, C. A. Bolle, F. d. l. Cruz, P. L. Gammel, C. S. Ogelsby, B. Batlogg, and D. J. Bishop, preprint.

[16] D. W. Braun, G. W. Crabtree, H. G. Kaper, A. E. Koshelev, G. K. Leaf, D. M. Levine, and V. M. Vinokur, Phys. Rev. Lett. (1996) (in press).

[17] G. W. Crabtree, G. K. Leaf, H. G. Kaper, V. M. Vinokur, A. E. Koshelev, D. W. Braun, D. M. Levine, W. K. Kwok, and J. A. Fendrich, Physica C (1996) (in press).

[18] M. C. Marchetti and D. R. Nelson, Phys. Rev. B 42 9938 (1990).

[19] A. Schmid, Phys. kondens. Materie 5 302 (1966).

[20] L. P. Gorkov and G. M. Eliashberg, Sov. Phys. – JETP 27 328 (1968).

[21] W. D. Gropp, H. G. Kaper, G. K. Leaf, D. M. Levine, M. Palumbo, and V. M. Vinokur, J. Comp. Phys. 123 (1996) (in press).

[22] C. A. Duran, P. L. Gammel, R. Wolfe, V. J. Fratello, D. J. Bishop, J. P. Rice, and D. M. Ginsberg, Nature (London) 357 474 (1992).

[23] M. Turchinskaya, D. L. Kaiser, F. W. Gayle, A. J. Shapiro, A. Roitburd, V. Vlasko-Vlasov, A. Polyanskii, and V. Nikitenko, Physica C 216 205 (1993).

[24] V. K. Vlasko-Vlasov, L. A. Dorosinskii, A. A. Polyanskii, V. I. Nikitenko, U. Welp, B. W. Veal, and G. W. Crabtree, Phys. Rev. Lett. 72 3246 (1994).

[25] U. Welp, T. Gardiner, D. Gunter, J. A. Fendrich, G. W. Crabtree, V. K. Vlasko-Vlasov, and V. I. Nikitenko, Physica C 235-240 241 (1994).

[26] C. A. Duran, P. L. Gammel, D. J. Bishop, J. P. Rice, and D. M. Ginsberg, Phys. Rev. Lett. 74 3712 (1995).

[27] U. Welp, T. Gardiner, D. O. Gunter, B. W. Veal, G. W. Crabtree, V. K. Vlasko-Vlasov, and V. I. Nikitenko, Phys. Rev. Lett. 74 3713 (1995).

[28] W. K. Kwok, U. Welp, G. W. Crabtree, K. G. Vandervoort, R. Hulscher, and J. Z. Liu, Phys. Rev. Lett. 64 966 (1990).

[29] F. Ternovskii and L. N. Shekhata, Sov. Phys. – JETP 35 1202 (1972).

[30] H. J. Jensen, Y. Brechet, and A. Brass, J. Low Temp. Phys. 74 293 (1989).